Analysis of diffusional stress relaxation in submicron Cu interconnect structures using the model with enhanced vacancy diffusivity in grain boundary region

I. Tsukrov, W. M. Grich & T. S. Gross
Department of Mechanical Engineering, University of New Hampshire, USA

Abstract

We propose the finite element simulation technique to model the process of diffusional creep and stress relaxation that occurs in Cu-damascene interconnects of integrated circuit devices in the processing stage. On the length scale of the interconnect lines (microns), the stress-induced mass flow constitutes the major mechanism of inelastic deformation. The mass flow problem is coupled to the stress analysis through vacancy flux and equilibrium vacancy concentration, allowing independently for the concentration profile and evolution of the stresses and strains in an iterative process to be solved. We decompose the total displacement field into the elastic part and the inelastic mass flow contribution. Performing the stress analysis in the configuration with accumulated inelastic displacements, we ensure that the shape of the interconnect line is compatible with external geometrical constraints throughout the simulation. This approach has been implemented in the software package that seamlessly integrates the problem-oriented code with the commercially available finite element program MSC.Marc. We apply the technique to model the Coble creep phenomenon by introducing the nanoscale grain boundary region having the thickness of the order of several layers of atoms. As an illustration, the problem of stress relaxation in a single grain subjected to prescribed displacements and tractions is examined.
Keywords: copper interconnects, diffusional creep, grain boundary, nanoscale deformation, finite elements.

1 Introduction

The fabrication of Cu-damascene interconnect lines has become an important field of research since early 1990's, when the first commercial samples were introduced. Much technological effort has been applied to reduce the feature size, which currently is on the order of a 100 nm (about 400 atomic radii). Operating on this length scale requires understanding of the impact of nanoscale mechanical behavior on reliability of conductors and interfaces. The major concerns arise due to the fabrication process, which includes reactive ion etching of a circuit pattern in a dielectric blanket, physical vapor deposition or chemical vapor deposition of a Ta-based diffusion barrier and deposition of copper. Thermal cycle from room temperature to 350-400 °C is used to anneal out the device damage from reactive ion etch. It is followed by chemomechanical polishing to flatten the layer and thus produce a planar layered structure. Figure 1 presents the atomic force microscope image of a real interconnect line manufactured by IBM.
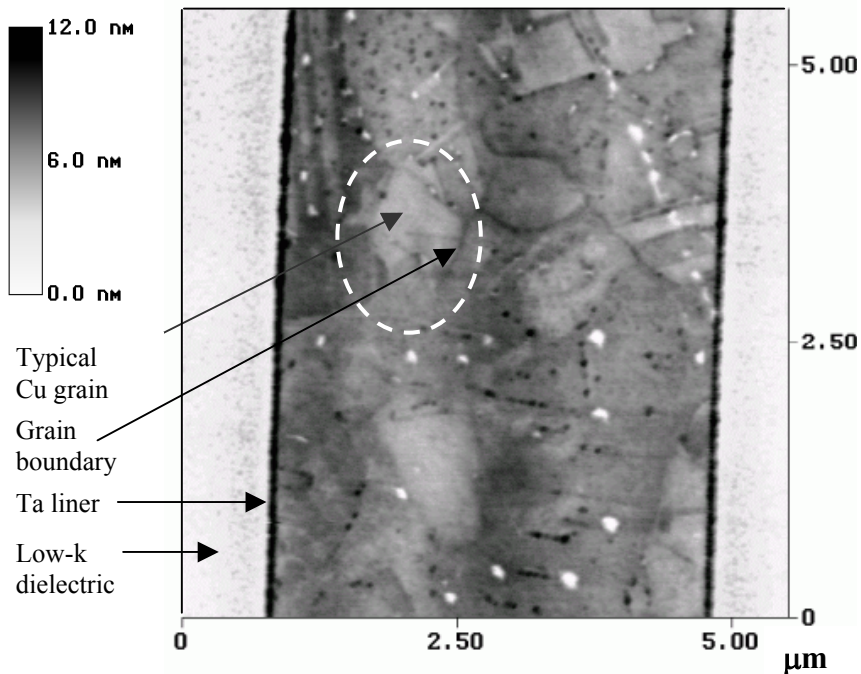

Figure 1:   Atomic force microscope topographical map of Cu-damascene.

During thermal processing, the conductor is subjected to considerable stresses from the thermal mismatch between the substrate, the dielectric and the diffusion barrier. The reliability of the conductors and interfaces depends on the state of stress. The deformation and stress relaxation in these nanometer scale structures is highly complex. We may assume that dislocation activity is not relevant at interconnect size scales and processing temperature ranges, as suggested, for

example, by Kobrinsky *et al.* [1]. The deformation may be attributed to the Cu-Cu grain boundary and Cu-Ta interfacial sliding, as well as to the material build up due to diffusional creep. The experimental background for this assumption was provided by Gross *et al.* [2], who developed an AFM method to measure out-of-plane deformation resulting from thermal cycling and applied this technique to observe the Cu-polyimide interconnect structure.

In this paper we develop the numerical method to predict the diffusion-based deformation that occurs in the process of interconnects fabrication. To describe this phenomenon adequately, the mathematical formulation is needed that accounts for the coupled nature of mechanical variables and concentration of species such as Cu atoms, vacancies and impurities. The decoupling of creep problem is achieved by its decomposition into the linear elasticity and mass flow subproblems, which are solved in an iterative process. Rzepka *et al.* [3] applied similar technique to a 3-D model of interconnect. We propose a different approach by utilizing the thermodynamical coupling equations and the concept of grain boundary region of finite thickness. A general discussion of lattice-based thermodynamics with respect to diffusional creep in interconnects was presented by Garikipati *et al.* [4]. Although our treatment is considerably simplified, it nevertheless gives adequate description of the creep/stress relaxation behaviour, and at the same time can be easily adapted to use with existing commercial finite element packages. We also devote special attention to the modelling of grain boundary regions, which are expected to be the major path of vacancy diffusion at the temperature ranges used in interconnects processing.

2   Decomposition of diffusional creep problem into elasticity and mass flow subproblems

The Arrhenius-type expression for equilibrium concentration of vacancies in the bulk at a given temperature is obtained from the minimum of Gibbs free energy ΔG_v written for dilute vacancy concentration (Porter and Easterling [5])

$$C_v^{eq} = \exp\left(-\Delta G_v / kT\right). \tag{1}$$

In this equation, k is Boltzmann constant and T is the absolute temperature. The Gibbs free energy can be expressed as $\Delta G_v = \Delta H_v - T\Delta S_v$, where ΔH_v and ΔS_v are the enthalpy and entropy of vacancy formation. The estimate for entropy of vacancy formation for Cu is typically given as $\exp\left(\Delta S_v / k\right) \cong 3$.

The enthalpy is given by $\Delta H_v = Q_f + \sigma_h \Omega$, where Q_f is the activation energy of vacancy formation, σ_h is the hydrostatic stress, and Ω is the atomic volume. The energy of vacancy formation at grain boundaries and free surfaces will be somewhat less due to reduced constraint.

Since there are no hydrostatic stress gradients in a uniaxially loaded solid, the vacancy concentration gradients that drive Nabarro-Herring and Coble creep

should not exist. Nabarro, Herring, and Coble all assumed that the equilibrium concentration in the region adjacent to the grain boundary is given by σ_n, the stress normal to the boundary. This can be rationalized by noting that the elastic constants of the grain boundary are different from that of the bulk as reported by Zhou and Huang [6] and other authors. Therefore, we assume that $\Delta H_v \cong Q_f + \sigma_n \Omega$ which is consistent with the implicit assumptions of Nabarro, Herring, and Coble.

We propose that vacancy creation or annihilation occurs instantaneously at grain boundaries and free surfaces, and that these surfaces are infinite sinks and sources of vacancies. Defining the temperature dependent stress-free vacancy concentration as $C_0 = \exp\left((T\Delta S_v - Q_f)/kT\right)$, the equilibrium vacancy concentration in the GB region is given by

$$C_v^{eq} = C_0 \exp\left(\sigma_n \Omega / kT\right). \tag{2}$$

We ignore the contribution of dislocations as vacancy sources and sinks since they are rarely observed in the interior of nanoscale grains (see Kong *et al.* [7] and references therein).

The vacancy diffusivity is given by $D_v = D_{v0} \exp\left(-Q_m /kT\right)$ where Q_m is the activation energy for vacancy motion. We assume that Q_m is less in a region adjacent to the grain boundary due to disorder near the interface and reduced elastic constraint. We choose the thickness of the enhanced diffusivity region as 3-4 monolayers, assuming the absence of impurities. We define the vacancy diffusivity at interfaces as $D_{v,gb} = D_{0gb} \exp\left(-Q_{m,gb}/kT\right)$ where $Q_{m,gb} = \alpha Q_m$ $(\alpha < 1)$. We are not aware of a precise method to measure the activation energy for vacancy motion through the grain boundary and will treat it as an adjustable parameter that may be affected by impurities, grain boundary roughness, crystallographic orientation and whether the opposing interface has similar diffusivity.

Neglecting the local vacancy relaxation strain (Hirth and Lothe [8]) the mass or atomic flux $\mathbf{j}_A$ is opposite to the vacancy flux $\mathbf{j}_v$:

$$\mathbf{j}_A = -\mathbf{j}_v. \tag{3}$$

The atomic flux field can be treated as the diffusive flow velocity field in a body that is statically fixed. The gradient of the mass flow velocity $-\nabla \mathbf{j}_v$ defines the rate of creep deformation

$$\dot{\varepsilon}_{cr} = -1/2\left(\nabla \boldsymbol{j}_v + \nabla \boldsymbol{j}_v^T\right). \tag{4}$$

The creep strains defined above are caused by diffusion mass flow due to stress field gradients. Assuming that total strain $\boldsymbol{\varepsilon}$ consists of elastic and creep components, the elastic part of the strain can be related to the total stress $\boldsymbol{\sigma}$ by Hooke's law

$$\boldsymbol{\sigma} = \boldsymbol{C} : (\boldsymbol{\varepsilon} - \boldsymbol{\varepsilon}_{cr}) \tag{5}$$

where $\boldsymbol{C}$ is the elastic stiffness matrix.

To analyze deformation of a grain assembly, we start with the uniform stress-free vacancy concentration C_0. Application of external load or prescribed displacements may result in stress gradients throughout the structure. This produces vacancy concentration gradients according to eqn (2). Vacancy diffusion leads to the accumulation of diffusion creep strains of eqn (4) and the evolution of stress field. The coupled vacancy diffusion – elasticity problem governed by eqns (2), (4)-(5) is solved by the finite element technique presented in the next section.

We implement the iterative approach to analyze the transient processes of diffusion creep or stress relaxation. It is assumed that with time step appropriately selected, we may adopt the staggered procedure on each iteration, i.e. solve the elasticity and mass flow subproblems independently, while holding the variables of another subproblem fixed.

The transient vacancy concentration subproblem is governed by the conservation law

$$\frac{\partial C_v}{\partial t} + \nabla \cdot \mathbf{j}_v = 0 \tag{6}$$

where vacancy fluxes $\mathbf{j}_v$ obey the Fick's constitutive equation

$$\mathbf{j}_v = -D_v \nabla C_v . \tag{7}$$

On each time step we integrate eqn (6) with fixed boundary vacancy concentrations given by eqn (2). The diffusive fluxes that occur during the time step are used to compute the creep strain increment $\Delta \boldsymbol{\varepsilon}_{cr}$ by integration of kinematic relation (4). The increment $\Delta \boldsymbol{\varepsilon}_{cr}$ is a component of total strain increment $\Delta \boldsymbol{\varepsilon}$. We choose the displacement as the independent variable, hence $\Delta \boldsymbol{\varepsilon}$ needs to be expressed in terms of displacement increments $\Delta \boldsymbol{u}$. Assuming small strain increments, we employ the relation $\Delta \varepsilon_{ij} = 1/2 (\Delta u_{i,j} + \Delta u_{j,i})$, where comma denotes partial differentiation with respect to the corresponding coordinate. The principle of virtual work may be written in incremental form as

$$\int_V \delta \boldsymbol{\varepsilon}^T : \boldsymbol{C} : (\Delta \boldsymbol{\varepsilon} - \Delta \boldsymbol{\varepsilon}_{cr}) dV = \Delta \boldsymbol{P} \tag{8}$$

where $\Delta \boldsymbol{P}$ is the increment of the externally applied load. This equation is the basis for the finite element formulation of mechanical subproblem.

3 Stress relaxation in 1D periodic row of square grains

We consider stress relaxation in a 2D (plane strain) grain array shown in Figure 2 subjected to applied strain $\varepsilon_x = 0.002$. The numerical values used in the computation are listed in Table 1.
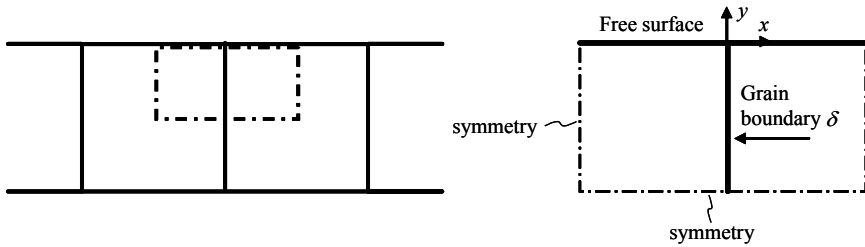
Figure 2:   Model of periodic square grain array used for validation of finite element procedure.

In the analysis of calculated results, we assume that the time dependence of average stress $\langle\sigma_{11}\rangle = 1/V \int_V \sigma_{11}dV$ can be approximated by Maxwell model relaxation function

$$\langle\sigma\rangle = \langle\sigma_0\rangle\exp(-t/\tau). \qquad (9)$$

In this equation, τ is the Maxwell model relaxation time defined through spring stiffness μ and dashpot viscosity η as $\tau = \eta/\mu$. We use the concept of relaxation time to characterize the time period of relaxation of average stress in the model, and to scale the time t in the graphs throughout the rest of this section.

Table 1:   Values of parameters used in the stress relaxation modeling of periodic grain array to compare numerical and theoretical predictions.

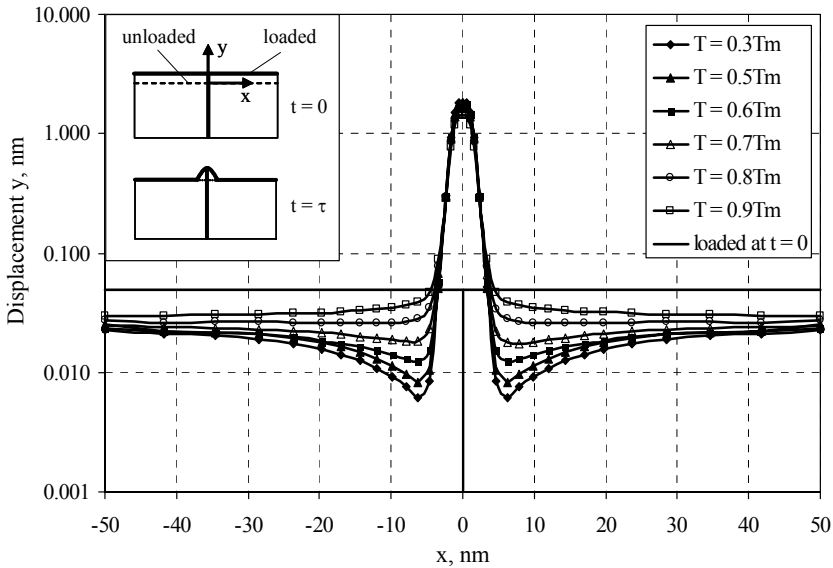| Parameter	Value
Grain width d	100 nm
Burgers vector b	0.25 nm
Grain boundary region thickness δ	1 nm
Atomic volume Ω	$1.18 \cdot 10^{-29}$ m^3
Melting temperature T_m	1356 K
Young's modulus E	128 Gpa
Poisson's ratio ν	0.33
Initial compressive stress on internal grain boundary σ_0	286.8 Mpa
Lattice vacancy diffusion pre-exponential D_{0L}	$2 \cdot 10^{-5}$ m^2/s
Lattice activation energy for vacancy motion $Q_{m,L}$	113.3 kJ/mole
Grain boundary vacancy diffusion pre-exponential $\delta_e D_{0gb}$	5e-15 m^3/s
Grain boundary activation energy for vacancy motion $Q_{m,gb}$	67.98 kJ/mole
Grain boundary activation energy for vacancy formation Q_f	83.7 kJ/mole

Figure 3:   Free surface profile at time $t = \tau$, with stress relaxation modeled at different temperatures. T_m is the melting temperature of copper.

Application of fixed strain ε_x results in initial uniform stress σ_0. Stress relaxation occurs as material flows towards the interfaces with the lowest magnitude of normal stress. For the structure under consideration, the smallest normal stress is at the free surface. The profiles resulting from the accumulation of material along the free surface at various temperatures are shown in Figure 3. The lump at the grain junction region results from material migration along the grain boundary (Coble mechanism). The height of the lump is approximately the same for all considered temperatures. It can be explained by the fact that the increased diffusivity at elevated temperatures is compensated by higher rate of vacancy flow (eqn 7). We also observe the increased accumulation of material along the free surface at high temperatures ($T > 0.5T_m$). This effect can be explained by contribution of vacancy diffusion through the grain interior (Nabarro-Herring mechanism).

Figure 4 shows the stress σ_{11} distribution along the internal grain boundary at different time instances. It can be seen that the stress relaxation occurs almost instantaneously at the junction between grain boundary and free surface, and gradually advances along the internal grain boundary. The stress distribution is shown at low and high temperatures, $T = 0.3T_m$ and $T = 0.7T_m$. The stress gradients are lower at high temperatures. This effect may be attributed to the contribution of Nabarro-Herring mechanism to stress relaxation. As seen in Figure 4, the difference in stress evolution at different temperatures is not substantial for a one-dimensional array of grains. Hence the relaxation of average

stress as a function of non-dimensional time t/τ can be plotted as a single curve, see Figure 5. The insets illustrate the evolution of stress field σ_{11} in the grain. Note that relaxation time τ is different for different temperatures, for example $\tau \sim 1\ s$ for $T = 0.5T_m$ and $\tau \sim 0.001\ s$ for $T = 0.7T_m$.

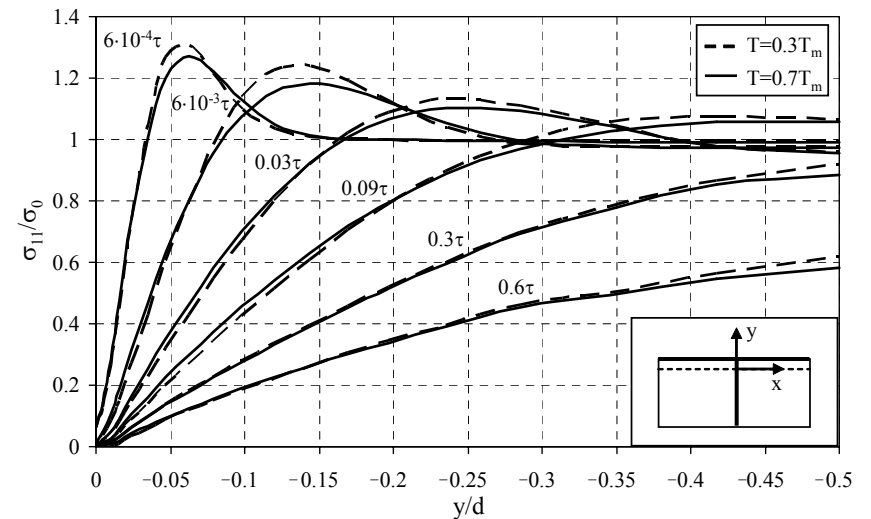Figure 4: Evolution of stress distribution along the internal grain boundary (x = 0) at temperatures $T = 0.7T_m$ (solid lines) and $T = 0.3T_m$ (dashed lines).
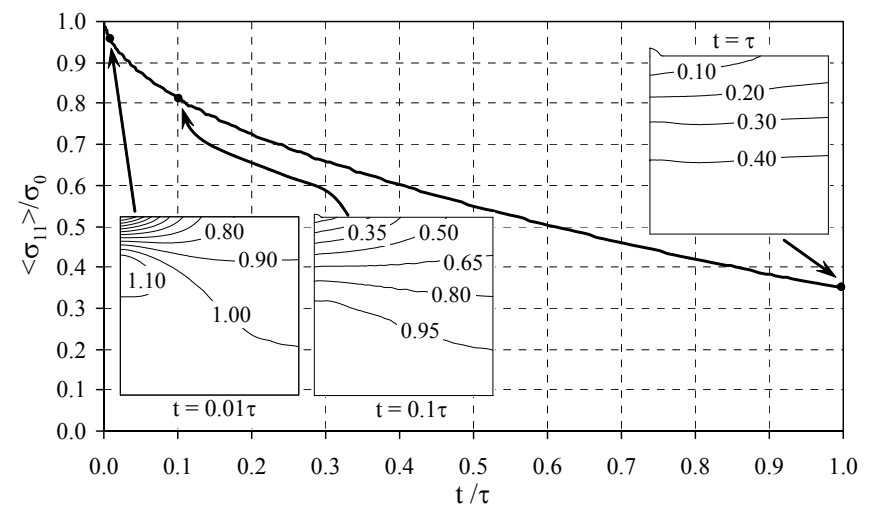

Figure 5: Relaxation of average stress $\langle\sigma_{11}\rangle$. Insets show the distribution of σ_{11} at selected time instances.

The numerical predictions are compared to the theoretical estimate based on the formula given by Frost and Ashby [9]

$$\dot{\gamma} = \frac{42\sigma\Omega}{kTd^2} D_L \left[1 + \pi \frac{\delta_e D_{gb}}{dD_L} \right] \qquad (10)$$

where $\dot{\gamma}$ is the shear strain rate, d is the grain width, δ_e is the effective thickness of grain boundary (on the order of magnitude of Burgers vector b) and σ is the applied stress. Note that the diffusivities D_L and D_{gb} in eqn (10) are based on the energy of both formation and motion of vacancies. They are different from the "vacancy motion only" diffusivities $D_{v,L}$ and $D_{v,gb}$ used in our finite element formulation which explicitly includes the vacancy formation energy in eqn (2) for stress dependence of vacancy concentration. We obtain the theoretical estimate of relaxation time by computing the dashpot viscosity from eqn (10) as $\eta = \sigma/\dot{\gamma}$. The shear strain rate in eqn (10) accounts for the contribution of both Nabarro-Herring and Coble mechanisms to creep rate, which is consistent with the numerical modeling approach of sections 2 and 3.

Figure 6 shows good agreement of theoretical and numerical predictions for relaxation time. The largest difference is in the temperature range 600-900 K.
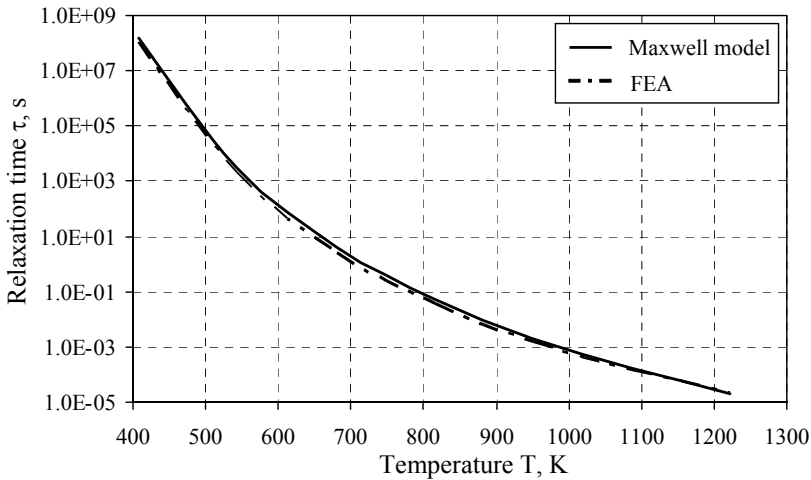

Figure 6:   Comparison of diffusion creep theoretical estimate of relaxation time τ to the finite element predictions.

4   Conclusions

The stress-induced mass flow constitutes the major mechanism of creep in Cu-damascene interconnects during thermal processing of integrated circuit devices.

This mechanism can be modelled by the iterative procedure which decouples the original creep problem into the static stress analysis and transient mass flow subproblems. Introduction of the grain boundary region with enhanced diffusivity into the finite element scheme allows direct modelling of effects associated with Coble creep behaviour.

Acknowledgements

References

[1]   Kobrinsky J., Thompson C. & Gross M., Diffusional creep in damascene Cu lines. *Journal of Applied Physics*, **89(1)**, pp. 91-98, 2001.
[2]   Gross T.S., Kamsah N. & Tsukrov I.I., Scanning probe microscopy generated out-of-plane deformation maps exhibiting heterogeneous nanoscale deformation resulting from thermal cycling of Cu-polyimide damascene interconnects. *Journal of Materials Research*, **16(12)**, pp. 3560-3566, 2001.
[3]   Rzepka S., Meusel E., Korhonen M. & Li C.-Y., 3-D finite element simulator for migration effects due to various driving forces in interconnect lines. *AIP Conference proceedings*, **491**, pp.150-161, 1999.
[4]   Garikipati K., Bassman L. & Deal M., A lattice-based micromechanical continuum formulation for stress-driven mass transport in polycrystalline solids. *Journal of the Mechanics and Physics of Solids*, **49(6)**, pp. 1209-1237, 2001.
[5]   Porter D.A. & Easterling K.E., *Phase Transformations in Metals and Alloys*, Chapman & Hall: London, 1992.
[6]   Zhou L.G. & Huang H., Are surfaces elastically softer or stiffer? *Applied Physics Letters*, **84(11)**, pp. 1940-1942, 2004.
[7]   Kong Q.P., Cai B., Lu L. & Lu K., The creep of nanocrystalline metals and its connection with grain boundary diffusion. *Defect and Diffusion Forum*, **188-190**, pp. 45-58, 2001.
[8]   Hirth J.P. & Lothe J., *Theory of dislocations*, Wiley-Interscience: New York, 1982.
[9]   Frost H.J. & Ashby M.F., Deformation-Mechanism Maps, The Plasticity and Creep of Metals and Ceramics, Pergamon Press: 1982.